Enhancing Floating Wind Turbine Reliability with Shared Damping Mooring

Tian, Haonan; Soltani, Mohsen N.; Colomés, Oriol

DOI
10.1109/ICRERA62673.2024.10815222

Publication date
2024

Document Version
Final published version

Published in
13th International Conference on Renewable Energy Research and Applications, ICRERA 2024

Enhancing Floating Wind Turbine Reliability with Shared Damping Mooring

Haonan Tian
Energy Department
Aalborg University
Denmark
hti@energy.aau.dk

Mohsen N. Soltani
Energy Department
Aalborg University
Denmark
sms@energy.aau.dk

Oriol Colomés
Civil Engineering Department
Technische Universiteit Delft
Netherlands
J.O.ColomesGene@tudelft.nl

2024 13th International Conference on Renewable Energy Research and Applications (ICRERA) | 979-8-3503-7558-9/24/$31.00 ©2024 IEEE | DOI: 10.1109/ICRERA62673.2024.10815222

***Abstract*—The reliability of mooring systems has long been a challenge for expanding floating wind turbines into deeper waters. The performance of the mooring system directly determines the service life and survival capability of floating wind turbines. To address this issue, our team has developed a shared damping mooring system. This system reduces the fatigue impact from operating sea conditions and effectively minimizes dragging damage at the fairlead. In this study, two widely used dampers were selected to construct the shared damping mooring system, and their effectiveness in enhancing the reliability of semi-submersible wind turbines was explored. Compared to traditional mooring methods, it was found that this shared damping approach can effectively increase the service life of mooring lines, reduce the local stress and tension levels at the fairlead, and improve the stability of semi-submersible wind turbines. Simulation results indicate that the shared damping mooring system can effectively alleviate fatigue damage, and the shaped memory alloy damper provides significant damping force under low-frequency environmental loads. This characteristic significantly enhances the floating foundation's stability and extends the mooring system's lifetime.**

Keywords—Semi-submersible Wind Turbine, Shared Damping Mooring, Lifetime Analysis, Shaped Memory Alloy Damper

I. INTRODUCTION

The reliability and service life of floating wind turbines (FWTs) have long been critical challenges in advancing deep-sea wind energy. The reliability of mooring systems directly impacts the stability and safety of these wind turbines. A survey on FWTs operations indicates that the accident rate for offshore structures throughout their operational lifetime can reach up to 96% (Ibrion et al., 2020). This highlights the significant influence of environmental loads on these incidents, including fatigue loads (Trubat et al., 2021), extreme storms (Yang and Kim, 2011), and tsunami impact damage. Such extreme conditions can lead to sudden shifts in the position and orientation of FWTs, drastically increasing the dynamic response of the platform (Bae and Kim, 2011). The remaining mooring lines may be subjected to excessive tension, potentially causing sequential failures. It is essential to design a reliable mooring system to maintain the required platform stiffness and mitigate the impact of wind and wave loads (Whitfield, 2019).

Numerous researchers have investigated the response of FWTs to mooring failures. Ahmed et al. (2016) explored the response of different mooring configurations following failure and discovered that floating platforms with symmetrical mooring line orientations provided stronger restoring forces. Bae et al. (2017) analyzed the performance of the OC4 DeepC-wind platform after a single mooring line failure, examining changes in the watch circle and the remaining line's fairlead tension. Li et al. (2018) studied the effects of mooring failures on winged beam-type FWTs, noting that significant drift motions caused by such failures could threaten nearby turbines. Ma et al. (2020) investigated the impact of extreme coherent gusts on the mooring lines of semi-submersible FWTs, finding that these gusts could significantly increase mooring line tension.

We propose a strategy of shared damping in mooring systems, aimed at enhancing the reliability of mooring systems under Fatigue Limit State (FLS) and Ultimate Limit State (ULS) conditions. The DNV OS-E301 (2010) standard defines three limit states in the design of offshore mooring lines: the Ultimate Limit State (ULS), which ensures that the maximum tension in the mooring line remains below the minimum breaking strength of the mooring components. The Fatigue Limit State (FLS), which represents the expected service life of the mooring line (typically 20 to 25 years for FWTs). (Pham, 2018) examined the interaction between ULS and FLS reliability, identifying a numerical correlation between overall reliability and these two design states. (Piscopo V, 2023) further clarified the design standards and requirements for limit states in FWTs design.

In current research on shared damping mooring systems, two promising materials for dampers have gained popularity: Shaped Memory Alloy (SMA) dampers and Seaflexible dampers (SFX). SMA dampers, leveraging the shape memory effect of the material, can return to their original shape under cyclic loads, offering excellent fatigue performance (Enferadi M H, 2019). The study by (Zuo H and Bi K, 2022) showcased the outstanding performance of SMA dampers in reducing vibrations in FWTs. The SFX damper, designed with special flexible materials, effectively absorbs energy through rubber

components and thermal resistance elements, reducing local stress concentrations (Thies P R, 2014).

In recent years, significant progress has been made in the research of mooring damping technology. Besides the damping methods commonly used for floating wind turbines (Haonan Tian, 2023), mooring damping technology has gradually become a more relied-upon option for offshore wind turbines. (Alnmr and Mayassah, 2023) explored a novel helical pile anchoring technique, which significantly enhances the stability of mooring lines. Furthermore, the shared mooring system design proposed by (Housner et al, 2024) demonstrates the potential for reducing complexity and improving damping effectiveness. (Cheng, 2024) studied a new hybrid single-point mooring system that effectively resists wave impacts, thereby protecting aquaculture facilities. These studies provide a solid foundation for enhancing the safety and efficiency of marine renewable energy systems, offering new perspectives and approaches for improving the safety and reliability of FWTs.

Our research team employed advanced numerical simulation tools, including Orcaflex, with the NPD wind spectrum and Jonswap wave spectrum, to perform detailed analyses of mooring systems under various sea states. This approach provides a comprehensive understanding of the characteristics of different damper combinations and offers a robust scientific foundation for designing mooring damping systems.

II. NUMERICAL MODEL

A. Mooring Modeling

In this study, Orcaflex was used to model both the traditional and the shared damping mooring systems of semi-submersible wind turbines (see Figure 1). The structural parameters of this unit come from the technical report of the NREL 5MW semi-submersible wind turbine (Robertson A, 2014). The motion equations of the entire FWTs system in the time domain can be written as:

$$\mathbf{F} = \&(\mathbf{M} + \mathbf{A}_\infty)\ddot{\mathbf{X}}(t) + \int_{-\infty}^{+\infty} \kappa(t-\tau)\dot{\mathbf{X}}(\tau)d\tau + \mathbf{C}\mathbf{X}(t) + \mathbf{K}(\mathbf{X}(t)) \quad (1)$$

In this context, $\mathbf{X}(t), \dot{\mathbf{X}}(t)$, and $\ddot{\mathbf{X}}(t)$ denote position, velocity, and acceleration vectors. M is the mass matrix, and $\mathbf{A}_\infty$ represents the added mass matrix at infinite frequency. The retardation function matrix $\mathbf{K}(t-\tau)$ is derived from frequency-dependent added mass and damping coefficients. $\mathbf{C}$ is the hydrostatic restoring matrix, and $\mathbf{K}(\mathbf{X}(t))$ is the nonlinear restoring matrix from the mooring system. $\mathbf{F}$ Includes external loads: wave excitation forces (first and second order), aerodynamic force, drag force, and mooring force. The mooring line's bending stiffness and hydrodynamic forces on its components are negligible (DNV, 2015), so only mooring tension is considered.

(Yan X，2023) provides the formulas used by Orcaflex to calculate the normal resistance, tangential resistance, horizontal tension, and vertical tension of the mooring elements:

$$\begin{aligned} \boldsymbol{\varepsilon} &= \frac{\boldsymbol{T}}{\boldsymbol{EA}} \\ \boldsymbol{F} &= \frac{1}{2}\boldsymbol{C_T}\boldsymbol{\rho}\boldsymbol{A}(\boldsymbol{V_c}\cos\boldsymbol{\theta})^2 \\ \boldsymbol{D} &= \frac{1}{2}\boldsymbol{C_N}\boldsymbol{\pi}\boldsymbol{\rho}\boldsymbol{A}(\boldsymbol{V_c}\sin\boldsymbol{\theta})^2 \end{aligned} \quad (2)$$

In the formula（2）, $\boldsymbol{\varepsilon}$ represents the elongation per unit length, E and A are the mooring lines' elasticity modulus and cross-sectional area, respectively. ρ denotes the seawater density, V_c is the speed of the seawater, C_N is the normal drag coefficient, and C_T is the tangential drag coefficient. The total mooring line tension T from Equation 2 can be regarded as the continuous integration of the mooring tensions of n segments. The local total tension $\boldsymbol{T_{i+1}}$ is the sum of the horizontal and vertical tensions.

$$\begin{aligned} \boldsymbol{T_{Xi+1}} &= \boldsymbol{T_{Xi}} - \boldsymbol{F_i}\cos\boldsymbol{\theta_i}(\boldsymbol{ds} + \boldsymbol{\varepsilon ds}) - \boldsymbol{D_i}\sin\boldsymbol{\theta_i}(\boldsymbol{ds} + \boldsymbol{\varepsilon ds}) \\ \boldsymbol{T_{Zi+1}} &= \boldsymbol{T_{Zi}} - \boldsymbol{F_i}\sin\boldsymbol{\theta_i}(\boldsymbol{ds} + \boldsymbol{\varepsilon ds}) + \boldsymbol{D_i}\cos\boldsymbol{\theta_i}(\boldsymbol{ds} + \boldsymbol{\varepsilon ds}) + \boldsymbol{P_i ds} \\ \boldsymbol{T_{i+1}} &= \sqrt{\boldsymbol{T_{Xi+1}^2} + \boldsymbol{T_{Zi+1}^2}} \end{aligned} \quad (3)$$

Among the functions, T_{Xi}, $T_{X(i+1)}$, T_{Zi}, and $T_{Z(i+1)}$ represent the horizontal and vertical tensions of the i th and i+1 th elements of the mooring line, respectively. D_i and F_i denote the normal and tangential drag forces acting on the i th mooring element. For mooring fatigue, damage is calculated using T-N curves. These curves define the number of cycles $N(T)$ required for the material to fail under a given range of effective tension. The T-N curves can be specified either parametrically or in tabular form. When specifying the curve parametrically, three parameters are required: m, k, and the reference breaking strength (RBS). D represents the damage value of the mooring system, and its function is represented as follows:

$$\boldsymbol{N} = \boldsymbol{k}\left(\frac{\boldsymbol{T}}{\boldsymbol{RBS}}\right)^{-\boldsymbol{m}} \quad (4)$$

$$\boldsymbol{D}(\boldsymbol{T}) = \frac{1}{\boldsymbol{N}(\boldsymbol{T})} \quad (5)$$

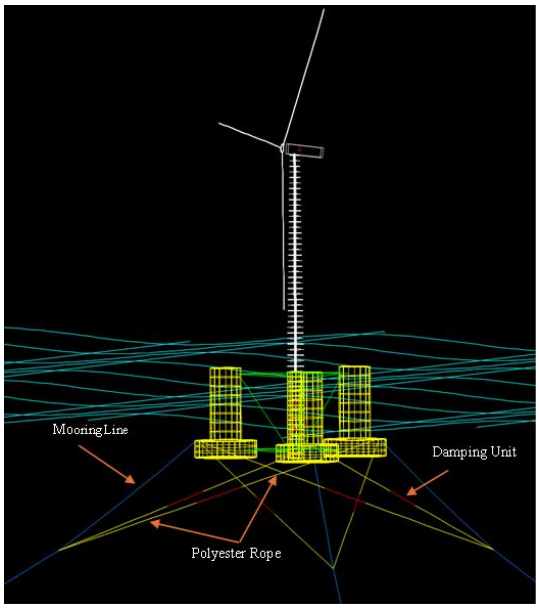

Fig1. Semi-submersible Wind Turbine with Shared Damping Mooring.

B. Shared Damping Characteristics

Referring to the work of Sheng Xu (2018), material damping is considered the optimal choice for partial damping in mooring

China Scholarship Council under Grant 202207940016.

systems. Material damping has minimal impact on the center of gravity and buoyancy of the floating body without significantly increasing its mass. Additionally, as a passive form of damping, material damping offers advantages such as fast response speed and ease of replacement and maintenance (Haonan Tian, 2023). The most used and well-known material dampers in underwater engineering include SMA dampers and SFX dampers.

(MH Enferadi, 2019) provided the characteristic formulas for SMA dampers:

$$F_{\mathrm{sh}\,j} = \begin{cases} F_{\mathrm{sh}\,j-1} + k_1(x_j - x_{j-1}) \\ A \times \sigma_s^{AM} + k_2(x_j - x_s^{AM}) \quad (F_{shj} > \text{Upper Plateau}) \\ A \times \sigma_f^{MA} + k_3(x_j - x_f^{MA}) \quad (F_{shj} < \text{Lower Plateau}) \end{cases} \tag{6}$$

$$\begin{cases} k_1 = \frac{A}{L} \times E_{SMA} \\ k_2 = \frac{A}{L} \times \frac{\sigma_f^{AM} - \sigma_s^{AM}}{\varepsilon_f^{AM} - \varepsilon_s^{AM}} \\ k_3 = \frac{A \times (\sigma_s^{MA} - \sigma_f^{MA})}{x_j - x_f^{MA}} \end{cases} \tag{7}$$

The advantages of SMA damper include super elasticity, high durability, and excellent energy dissipation capability. It offers superior corrosion resistance and fatigue performance in harsh marine environments. Additionally, its stiffness can be adjusted with temperature, making it highly effective in vibration control and an ideal choice for enhancing the stability of offshore structures.

(Thies P R, 2014) provided the restoring force characteristics (formula 8) for the SFX damper. The energy dissipation of the SFX damper can be quantified through numerical integration of the area enclosed by the load-extension curve.

$$E = \int_a^b f(x)dx - \int_a^b g(x)dx \tag{8}$$

Here, $f(x)dx$ represents the upper part of the load-extension curve, $g(x)dx$ represents the lower part, and the parameters a and b are the values at the intersection points of the curves. Using the trapezoidal rule, $f(x)dx$ can be expressed as:

$$\int_a^b f(x)dx \approx (b-a)\left[\frac{f(a)+f(b)}{2} + \sum_{k=1}^{n-1} f\left(a + k\frac{b-a}{n}\right)\right] \tag{9}$$

The advantages of the SFX damper lie in its ability to provide a soft response under normal operating conditions, allowing the necessary movement of floating devices, while exhibiting high stiffness in extreme load conditions (such as during storms). This dual-response capability helps to reduce peak loads in conventional mooring systems, extend the system's lifetime, and enhance overall reliability. Additionally, the material characteristics of the SFX damper make it excellent in terms of fatigue and creep performance, meeting the demands of long-term applications.

III. Cases Research

The design of the mooring system typically employs the Norwegian Petroleum Directorate (NPD) wind spectrum (DnV-GL, 2018a), with wave simulations based on the Jonswap spectrum. This study utilized Orcaflex to develop multiple finite element models of semi-submersible wind turbines, considering configurations both with and without mooring damping systems. The analyzed mooring configurations included traditional mooring, shared mooring with polyester ropes, shared mooring with shaped memory alloy (SMA) dampers, and shared mooring with SFX dampers. The analysis drew on weather data from the MET wind turbine test center within the ERA5 dataset, situated in waters exceeding 200 meters in depth, suitable for testing the mooring chains of semi-submersible turbines. In marine environments, wave-induced loads are primarily carried by mooring lines aligned with the wave direction, leading to significant tension fluctuations and rapid degradation over time. Therefore, the subsequent analysis will focus on this specific mooring line.

A. Selection of Sea States

Real sea states exhibit different characteristics in various regions, which can also have varying impacts on FWTs. The distribution of wind speed, wave height, and period data at the wind farm from 2019 to 2023 is shown in Figure 2. Significant fluctuations in wind and wave conditions were observed at Norway's MET wind turbine test center, with a maximum wave height of 6.2 m, maximum wind speed of 27.5 m/s, and maximum critical wave period of 20 s.

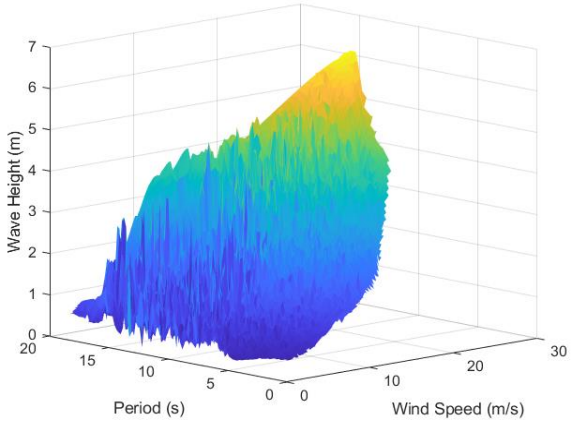

Fig2. Distribution of Wind Speed, Wave Height, and Period Data for the 5 Years from 2019 to 2023.

The working sea state combinations for this offshore wind farm were identified through probability density plots (see Figures 3 and 4).

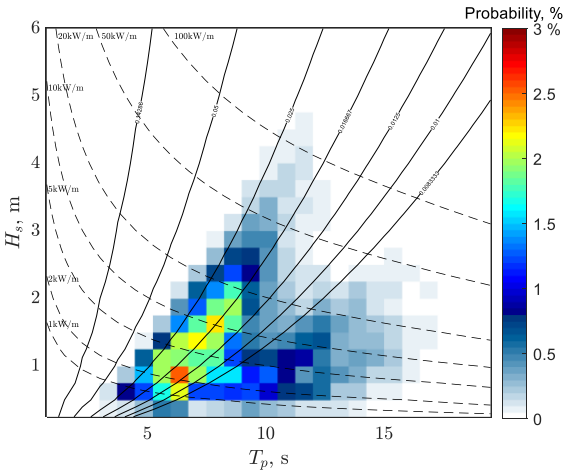

Fig3. Probability Density Plot of Wave Height and Period.

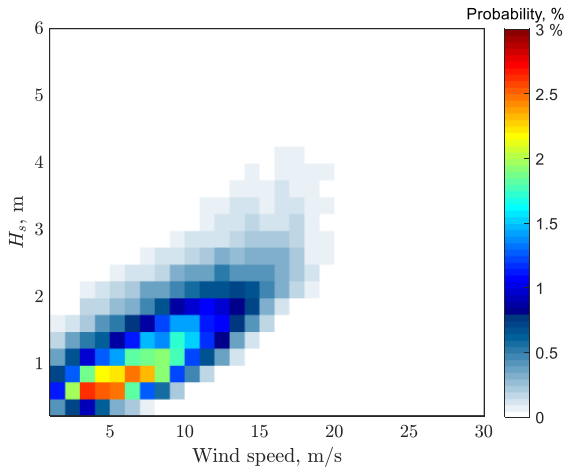

Fig4. Probability Density Plot of Wind Speed and Wave Height.

Using the environmental contour method (Haselsteiner A F, 2021), extreme sea state combinations for a 50-year return period were predicted, as shown in Table 1. These extreme sea state combinations were uniformly extracted from the boundaries of the environmental probability density plots to assess the performance of the damping systems.

Table 1: Extreme Sea State Combination Data

Order	Wave Height (m)	Period (s)	Wind speed (m/s)
LC 1	6.5	13	27
LC 2	6.3	13.5	28
LC 3	4.3	22	29
LC 4	2.3	23.5	25
LC 5	0.5	22.5	15
LC 6	4.7	11	11.5
LC 7	5.8	13	17
LC 8	6	17	20

B. Hydrodynamic Characteristics of Mooring System

An increasing number of researchers are focusing on the contribution of mooring damping technology to FWTs. Depending on different working principles and scenarios, the response speed and damping effectiveness of material damping are highly regarded. Based on the work of (MH Enferadi, 2019) and (Thies P R, 2014), the restoring force characteristics of the SMA and SFX dampers were reproduced, as shown in Figures 5 and 6. These dampers, functioning as damping units, were cross connected to the mooring lines using polyester fiber ropes (see Figure 1). In the Orcaflex comparison group, the four mooring systems and their corresponding RAO (Response Amplitude Operator) frequencies are listed in Table 2.

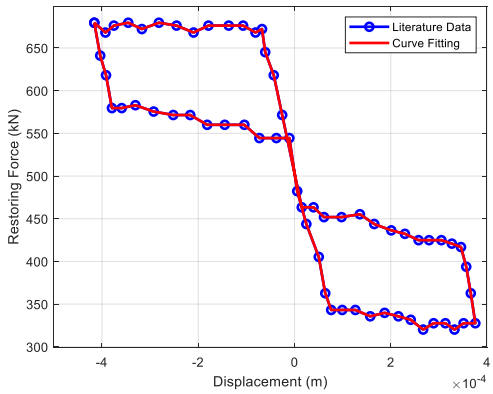

Fig5. SMA Damping Force follows the Displacement.

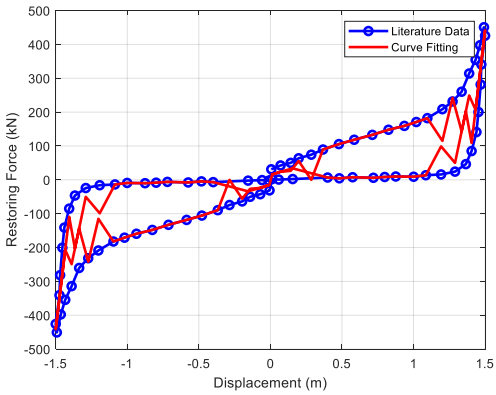

Fig6. SFX damping Force follows the displacement.

Table 2: Four Mooring Systems and RAO Frequencies

Object	Surge frequency (Hz)	Heave frequency (Hz)	Pitch frequency (Hz)
Traditional Mooring	0.01117	0.08056	0.04819
With Polyester Rope	0.01282	0.08053	0.05061
With SMA Damper	0.01299	0.08053	0.05062
With SFX Damper	0.01285	0.08054	0.05058

According to the simulation results, these four types of mooring systems have an impact on the RAO motion frequency of the floating platform. Among them, polyester fiber ropes have a smaller impact on the system's motion frequency compared to the other two damping combinations.

IV. Evaluation and Analysis

A. Impact of Operating Sea States

To evaluate the impact of operating sea states on the mooring system's lifetime, operating conditions (Load case 1 to Load case 45) with a probability greater than 1% were selected from

Figures 3 and 4. Fatigue analysis was conducted on the four mooring configurations, resulting in the mooring line lifetime distribution shown in Figure 7. Compared to the traditional mooring method, the other three configurations can extend the lifetime by sharing wind and wave loads. Among these, the SMA mooring system exhibits a longer lifetime at the FOWT fairlead than the other three types, while the polyester fiber rope mooring system significantly outperforms traditional mooring methods. SFX dampers reduce damage along the mooring line and significantly extend its lifetime.

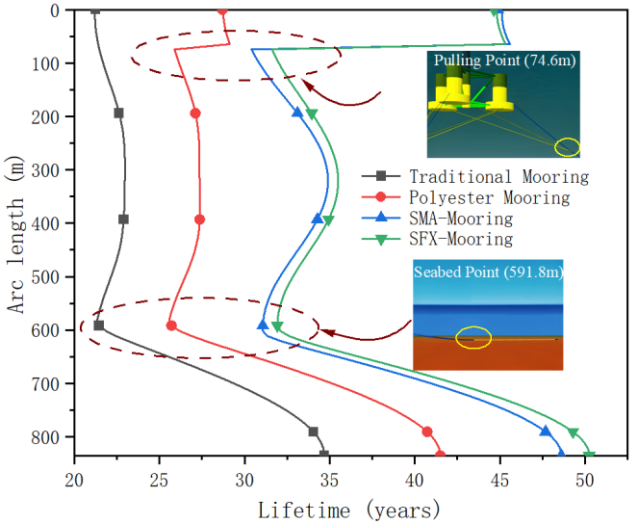

Fig7. Lifetime Distribution of Mooring Lines for Four Mooring Configurations.

Comparing the damage caused by high-probability sea states to the four mooring systems in detail, Figure 8 shows the mooring damage at the mooring dangerous position. It was observed that eight operating conditions cause significant damage to the anchor chains of the traditional mooring system, with their sea state parameters and durations listed in Table 3. The comparison shows that SMA dampers can effectively reduce the damage caused by these sea states, with the maximum reduction in damage observed in Fatigue Case 14, which decreased by 0.43.

Table 3: Operating Conditions with More Severe Damage

Fatigue Case	Sea State Combine			Last Time (h)	Damage
	Wave Height (m)	Period (s)	Wind Speed (m/s)		
10	0.5	10.5	4.5	396.7	0.268
11	0.5	10.5	7.5	282.1	0.296
13	0.5	13.5	1.5	76.4	0.364
14	0.5	13.5	4.5	137.4	0.43
32	1.5	13.5	1.5	23	0.22
33	1.5	13.5	4.5	75.86	0.325
35	1.5	13.5	10.5	157.56	0.41
40	1.5	7.5	16.5	45.2	0.206

The lifetime distribution chart for the four mooring methods indicates that, for traditional mooring, the most critical locations remain the fairlead and the seabed anchor point. For the shared damping mooring method, the first critical location appears at the connection between the anchor chain and the damping mechanism, with the second critical location also being the seabed anchor point. Table 4 shows four mooring types of dangerous positions and lifetime.

Table 4: Dangerous Locations Lifetime for Four Mooring Types

Object	Traditional Mooring (years)	Polyester (years)	SMA (years)	SFX (years)
Location 1	21.2	25.9	30.4	31.6
Location 2	21.3	25.5	31.1	31.9

Based on the lifetime data in Table 3 and the damage formula 5, it is evident that the maximum damage for traditional mooring occurs at the fairlead, while for the other three shared damping mooring methods, the maximum damage occurs at the binding point.

The analysis of high-damage sea states found that the maximum damage occurs when the wind speed is close to the rated wind speed. However, this is not the only condition leading to high damage. Significant damage also occurs when the critical wave period is 10.5 s or 13.5 s, in addition to the wind speed. During these periods, the wave frequency is very close to the RAO frequency of the semi-submersible wind turbine (Wang S, 2024), which is undoubtedly a major factor contributing to increased system sway and vibration. Based on these two conditions, the longer the duration of the sea state, the greater the resulting damage.

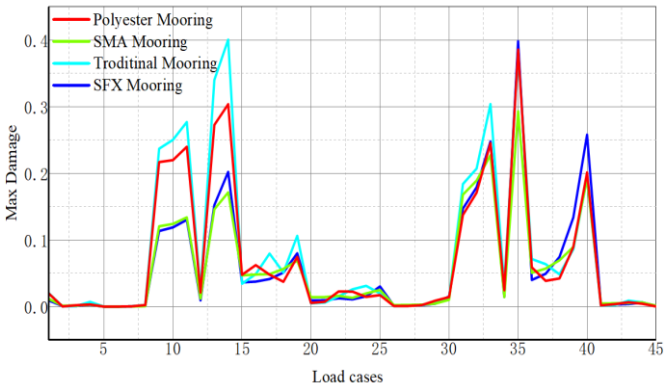

Fig8. The Comparison of Operational Damage under Different Mooring Schemes.

In the working sea states of the FWTs shown above, the critical wave period ranges for sea states 1 to 45 are from 0.5s to 3.5s. From the comparison of the performance of the four systems under operating sea states in the above chart, it can be observed that the traditional mooring method generally performs poorly in terms of damage under most sea states. The polyester mooring system experiences less damage than the traditional mooring when the critical wave period is less than 1 s. When the critical wave period is between 1.5s and 2.5s, the

performance of the SMA mooring system is superior to the other three types.

The maximum tension in the mooring system is shown in Figure 9. Comparing the maximum tension locations under the operational sea states for the four systems reveals that there is no significant difference between the SFX, SMA damping scheme, and the traditional mooring method. In engineering practice, local tension and stress levels can be comparable to the traditional mooring method through proper connection design (such as hinged connections). Based on the above life and damage results, SFX damping has a more obvious improvement effect on mooring system fatigue. Polyester fiber ropes generate the least tension on the mooring lines because they provide lower damping force and stiffness.

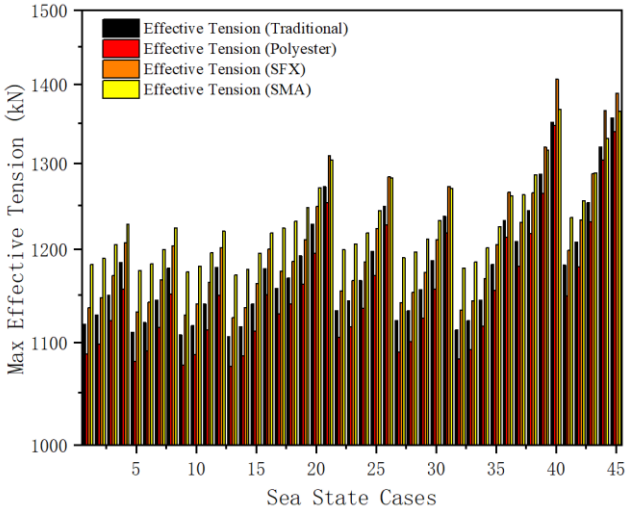

Fig9. Comparison of Maximum Effective Tension under Operational Conditions.

B. *Impact of Extreme Sea States*

The SMA Mooring system demonstrated excellent energy dissipation characteristics in analyzing operating sea states. However, for deep-sea FWTs, extreme sea states pose a greater threat. Research by (Adebayo Ojo， 2022) indicates that the impact of extreme sea states on mooring fatigue is insignificant. Therefore, this study aims to assess the threat posed by the extreme sea states by evaluating the pitch angle of the floating foundation and the effective tension in the mooring lines and to compare the advantages of different types of damping. By establishing extreme wind and wave combination cases in simulations (Case 1 ~ Case 8), the floating foundation's pitch angle varies significantly under extreme sea states (see Figure 10). Other mooring failures or in-plane displacements of the platform can be evaluated through local stress levels.

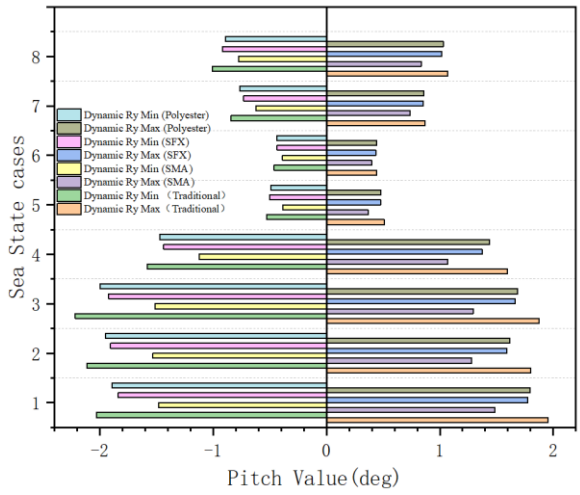

Fig10. The Pitch Angle of the Mooring System under Extreme Sea States.

Analysis of the eight extreme sea state scenarios in Figure 10 reveals that the pitch angle of the floating foundation changes most significantly with the traditional mooring method. Additionally, the performance of the Polyester mooring and SFX mooring systems is similar, both effectively suppressing changes in pitch angle. SMA mooring is the best choice for preventing floating foundations from overturning under extreme sea states. Among the eight scenarios, the traditional mooring system in Case 3 exhibited the largest pitch angle of 4°, while the SMA mooring system in Case 5 showed the smallest change, with a pitch angle of only 0.76°. In the comparison of maximum bend moment (Figure 11), the Case 3 sea state combination was the most dangerous, resulting in a maximum bending moment of 0.24 kN • m at the top of the anchor chain for the traditional mooring method. In contrast, the SMA and SFX mooring systems performed well under all eight extreme sea states, while the polyester mooring system effectively reduced the maximum bending moment at the top of the mooring line and prevented FWTs instantaneous capsizing.

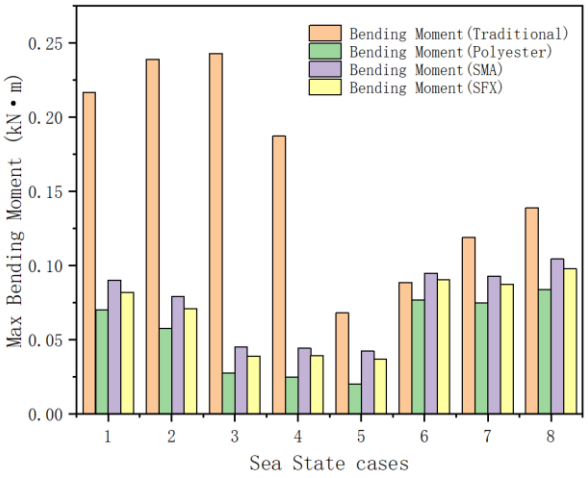

Fig11. The Maximum Bending Moment of the Mooring System under Extreme Sea States.

Similarly, we conducted a tension analysis of the four mooring systems under extreme sea states and found that the trends in the mooring control group were consistent with those observed under fatigue sea states. Polyester mooring can effectively reduce local tension and stress under extreme sea states. Under high energy environmental loads, SMA damping can reduce the pitch angle by providing higher stiffness and preventing FWTs rollover. This is the main reason why the maximum bending moment of this mooring method is slightly higher than that of the other two.

C. *Damping Performance under Extreme Sea State*

To closely examine the impact of wind and wave variations on damping force under extreme sea states, a damping force vs. sea condition variation chart, as shown in Figure 12. By comparing the differences between SMA and SFX damping forces in specific sea states, it can be observed that in LC3, LC6, and LC8 conditions, the maximum damping force provided by SFX is higher than that of the SMA dampers. In the remaining extreme conditions, the maximum damping force values are very close. To more intuitively capture the changes in damping force, probability density histograms of damping force under 8 extreme sea states were also plotted (Figure 13).

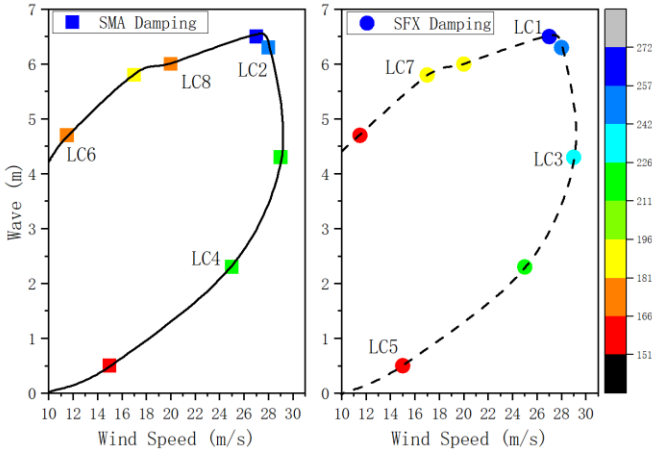

Fig12. Damping Force Distribution under Extreme Sea State.

In analyzing the damping force distribution of SMA and SFX, we found that as wave height and wind speed increase, the distribution of both SMA and SFX exhibits a noticeable rightward shift, indicating that the damping force is concentrated in higher value ranges, with an accompanying increase in distribution width. This shift reflects the intensified fluctuation of damping force under conditions of high wave height and strong wind, leading to a more dispersed distribution. Additionally, the impact of wind speed on SFX is particularly significant, with SFX's distribution becoming broader than SMA's under high wind conditions, indicating a wider range of damping force values. In contrast, an increase in wave height generally causes the peak of the damping force distribution to shift rightward, while changes in wave period affect the width and position of the peak. Long-period waves tend to result in a smoother and broader damping force distribution, whereas short-period waves cause the damping force to concentrate in higher value ranges. These findings suggest that variations in wave height, wind speed, and period under different extreme sea states significantly influence damping force distribution, with SFX's damping characteristics being more suitable for complex and variable extreme sea states.

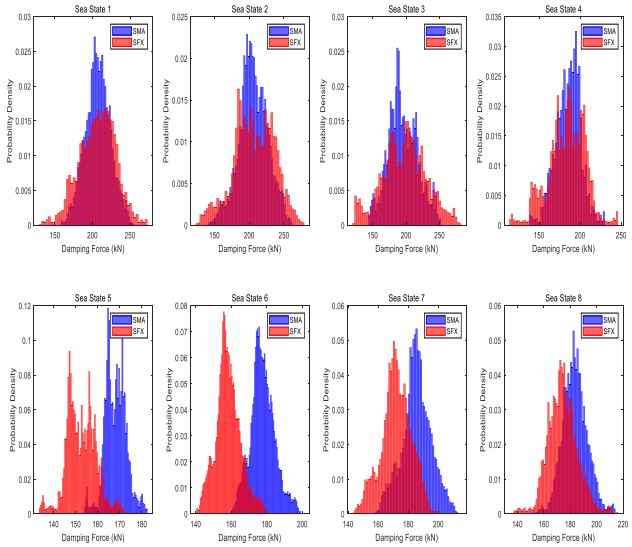

Fig13. Probability Density Histogram of Damping Force under Extreme Sea States.

V. CONCLUSION AND OUTLOOK

The study conducted a comparative analysis of the performance of traditional mooring systems and shared damping mooring systems under different Sea States, validating the effectiveness of the shared damping strategy in enhancing the reliability of mooring systems for floating wind turbines. Through comparative analysis of the performance of several shared damping schemes versus traditional mooring schemes, we can draw the following key conclusions：

1. The shared damping system effectively reduces fatigue damage to the mooring system in operational sea states. In extreme sea states, it reduces local tension by about 6% and bending moments by approximately 87%, significantly lowering the risk of structural failure.
2. The SFX damper adapts well to changes in the operational sea states, providing a wider range of damping forces. This adaptability extends the lifetime of the mooring system, with an improvement of about 53%, and offers greater damping force for the floating foundation under extreme conditions.
3. The SMA damper has significant advantages in preventing capsizing, effectively controlling the pitch angle of the floating platform, and reducing the risk of capsizing under extreme sea states by up to 24.06%. This feature enhances the overall safety and stability of the system.

Outlook:

Future research and development should focus on further optimizing the design of shared damping systems to better balance cost and reliability, particularly in integrating the advantages of SMA and SFX dampers under extreme Sea States. Moreover, as the scale of FWTs expands, more empirical data will be crucial for verifying and refining these system designs. Long-term testing under real Sea States will help ensure the stability and safety of these systems under various extreme conditions, ultimately driving the large-scale application of these technologies and providing solid technical support for the development of offshore wind power.

ACKNOWLEDGMENT

This paper is supported by a scholarship from the China Scholarship Council under Grant 202207940016.

REFERENCES

[1] Ibrion, M., Paltrinieri, N., Nejad, A.R., 2020. Learning from failures: accidents of marine structures on Norwegian continental shelf over 40 years time period[J]. Eng. Fail. Anal. 111, 104487. Trubat, P., Molins, C., Alarcon, D., et al., 2021.

[2] Mooring Fatigue Verification of the WindCrete for a 15 MW Wind Turbine[C]//International Conference on Offshore Mechanics and Arctic Engineering. American Society of Mechanical Engineers, 84768. V001T01A017.

[3] Yang, C.K., Kim, M.H., 2011. The structural safety assessment of a tie-down system on a tension leg platform during hurricane events. J. Ocean Syst. Eng. 1 (4), 263–283.

[4] Bae, Y.H., Kim, M.H., Kim, H.C., 2017. Performance changes of a floating offshore wind turbine with broken mooring line[J]. Renew. Energy 101, 364–375.

[5] Whitfield, S., 2019. Lessons Learned from the Big Foot Mooring Incident. Retrieved from. https://jpt.spe.org/lessons-learned-big-foot-mooring-incident.

[6] Ahmed, M.O., Yenduri, A., Kurian, V., 2016. Evaluation of the dynamic responses of truss spar platforms for various mooring configurations with damaged lines. Ocean Eng. 123, 411–421.

[7] Bae, Y., Kim, M., Kim, H., 2017. Performance changes of a floating offshore wind turbine with broken mooring line. Renew. Energy 101, 364–375.

[8] Li, Y., Zhu, Q., Liu, L., Tang, Y., 2018. Transient response of a SPAR-type floating offshore wind turbine with fractured mooring lines. Renew. Energy 122, 576–588.

[9] Ma, G., Zhong, L., Zhang, X., Ma, Q., Kang, H.-S., 2020. Mechanism of mooring line breakage of floating offshore wind turbine under extreme coherent gust with direction change condition. J. Mar. Sci. Technol. 25, 1283–1295.

[10] DNV Offshore Standard - Position Mooring, 2010. DNV OS-E301.

[11] Yan X, Chen C, Yin G, et al. Numerical investigations on nonlinear effects of catenary mooring systems for a 10-MW FOWT in shallow water[J]. Ocean Engineering, 2023, 276: 114207.

[12] DNV GL, 2018a. Energy transition outlook 2018. In: Maritime Forecast to 2050. https://eto.dnvgl.com/2018/maritime.

[13] Pham, H.H., 2018. Methodology for total reliability evaluation of the mooring lines of floating offshore structures. In: The Vietnam Symposium on Advances in Offshore Engineering. VSOE), Hanoi.

[14] Piscopo V, Scamardella A. Incidence of wind spectrum and turbulence intensity on the design of mooring systems for floating offshore wind turbines[J]. Ocean Engineering, 2023, 290: 116377.

[15] Enferadi M H, Ghasemi M R, Shabakhty N. Wave-induced vibration control of offshore jacket platforms through SMA dampers[J]. Applied Ocean Research, 2019, 90: 101848.

[16] Zuo H, Bi K, Hao H, et al. Numerical study of using shape memory alloy-based tuned mass dampers to control seismic responses of wind turbine tower[J]. Engineering Structures, 2022, 250: 113452.

[17] Thies P R, Johanning L, McEvoy P. A novel mooring tether for peak load mitigation: Initial performance and service simulation testing[J]. International Journal of Marine Energy, 2014, 7: 43-56.

[18] Ojo, A., Collu, M., & Coraddu, A. (2022). Multidisciplinary design analysis and optimization of floating offshore wind turbine substructures: A review. Ocean Engineering, 266(Part 1), 112727. ISSN 0029-8018. https://doi.org/10.1016/j.oceaneng.2022.112727

[19] Haselsteiner A F, Coe R G, Manuel L, et al. A benchmarking exercise for environmental contours[J]. Ocean Engineering, 2021, 236: 109504.A benchmarking exercise for environmental contours.

[20] Wang S, Moan T. Analysis of extreme internal load effects in columns in a semi-submersible support structure for large floating wind turbines[J]. Ocean Engineering, 2024, 291: 116372.

[21] Xu S, Ji C, Soares C G. Experimental study on taut and hybrid moorings damping and their relation with system dynamics[J]. Ocean Engineering, 2018, 154: 322-340.

[22] Enferadi M H, Ghasemi M R, Shabakhty N. Wave-induced vibration control of offshore jacket platforms through SMA dampers[J]. Applied Ocean Research, 2019, 90: 101848.

[23] Thies P R, Johanning L, McEvoy P. A novel mooring tether for peak load mitigation: Initial performance and service simulation testing[J]. International Journal of Marine Energy, 2014, 7: 43-56.G. Eason, B. Noble, and I. N. Sneddon, “On certain integrals of Lipschitz-Hankel type involving products of Bessel functions,” Phil. Trans. Roy. Soc. London, vol. A247, pp. 529–551, April 1955.

[24] Robertson A. Definition of the Semisubmersible Floating System for Phase II of OC4[R]. NREL Technical Report, NREL/TP-5000-60601, 2014.

[25] Alnmr A, Mayassah M. Innovations in offshore wind: reviewing current status and future prospects with a parametric analysis of helical pile performance for anchoring mooring lines. *Journal of Marine Science and Engineering*, 2023; 12(7): 1040.

[26] Housner S, Hall M, Tran TT, de Miguel Para B. Shared mooring system designs and cost estimates for wave energy arrays. *Renewable Energy*, 2024; 189, 123-135.

[27] Cheng Y, Gong J, Zhang J. Hydrodynamic investigation on a single-point moored offshore cage-wave energy converter hybrid system. *Applied Ocean Research*, 2024; 126, 102305.

[28] Tian, H., Soltani, M. N., Nielsen, M. E. Review of floating wind turbine damping technology. *Ocean Engineering*, 2023; 278, 114365.

